Lateral composition modulation in InAs/GaSb superlattices

D. W. Stokes,[a] R. L. Forrest,[b] J. H. Li, and S. C. Moss
Department of Physics, University of Houston, Houston, Texas 77204

B. Z. Nosho,[c] B. R. Bennett, and L. J. Whitman
Naval Research Laboratory, Washington, DC 20375

M. Goldenberg
SFA, Inc., Largo, Maryland 20774

(Received 22 August 2002; accepted 24 October 2002)

We report the analysis of lateral composition modulation in $(InAs)_m/(GaSb)_m$ superlattices by x-ray diffraction. Vertical and lateral satellite peaks for a 140 period structure were observed. The lateral modulation wavelength, average superlattice composition, and vertical superlattice wavelength were determined. The lateral modulation was observed only along one in-plane direction resulting in quantum wire-like structures along the $[1\bar{1}0]$ direction. The unconventional structure of the lateral composition modulation, in which the stacking of the layers leads to a doubling of the vertical superlattice period, is discussed. © *2003 American Institute of Physics.*
[DOI: 10.1063/1.1529291]

I. INTRODUCTION

Lateral composition modulation (LCM) is the spontaneous formation of phase-separated, self-organized periodic structures parallel to the surface during epitaxial growth of semiconductor films. Recent studies have demonstrated LCM in a number of III–V semiconductor ternary alloys, both in ABC_2 single-layer structures[1,2] and in vertical short-period superlattice (SPS) structures consisting of two lattice mismatched components $(AB)_m/(CD)_n$, i.e., $(InP)_m/(GaP)_n$,[3,4] where m and n denote the number of atomic monolayers. Typical lateral wavelengths range from 100 to 400 Å.[5,6] LCM has been shown to have profound consequences on the physical properties of these semiconductor systems, e.g., band gap reduction, valence-band splitting, and in-plane anisotropy,[7] all of which may be exploited for optoelectronic applications. In particular, light emitting diodes and lasers with compositionally modulated active regions have already been fabricated and have demonstrated modified materials performance in comparison to conventional quantum well lasers.[8–10]

The causes of LCM are currently under debate, but it is generally agreed that there is a kinetic process in which surface diffusion, including a gradient term, together with strain lead to thickness undulation and composition modulation.[11] The detailed combination of these different effects is material dependent, and so it is possible that different mechanisms predominate in single-layer versus SPS structures.[12]

In this work we report the x-ray diffraction analysis of LCM in InAs/GaSb superlattices (SL). These superlattices are important because of their use in optoelectronic applications such as midwave infrared detectors[13] and lasers.[14]

[a]Electronic mail: dstokes@uh.edu
[b]Present address: University of Houston-Downtown, Department of Natural Sciences, Houston, TX 77002.
[c]Present address: HRL Laboratories, LLC, Malibu, CA 90265.

II. EXPERIMENT

A 140 period $(InAs)_{13}/(GaSb)_{13}$ superlattice structure was grown by molecular beam epitaxy on GaSb (001) substrates, with a 2000 Å GaSb buffer and a 100 Å InAs cap. The SL was intentionally grown with InSb interfacial bonds. Details of the growth are given elsewhere.[15] The superlattice was grown with a vertical wavelength of approximately 80 Å, both InAs and GaSb layers being nominally 40 Å, i.e., this is not a SPS structure, in which each layer is only a few monolayers thick. Employing high-resolution x-ray diffraction (XRD) we are able to describe the average morphology of the structure, including the vertical and lateral modulation wavelengths, the strain in the layers, and the orientation of the LCM. This article will discuss the observed LCM morphology and the causes of the LCM.

III. RESULTS

Figure 1 shows a cross-sectional scanning tunneling microscopy (XSTM) image in the [110] projection for the entire vertical height of the superlattice where images of periods (a) 1–45, (b) 32–84, (c) 58–117, and (d) 84–137 are shown. Lateral thickness undulations are evident in both the InAs and GaSb layers, dark and bright regions, respectively, but are more prominent in the InAs layers. From these images it is clearly seen that it took a few periods of growth before the modulation was initiated, and the peak-to-trough height increased as the growth continued until about 40 periods, where they became regular; beyond about 80 periods, the modulation became quite irregular. This is the clearest image of laterally organized thickness undulations in a SL reported to date.[16] XSTM images indicate that no lateral undulations occur in the orthogonal plane.[15,16]

Thickness undulations in superlattice bilayers have been a leading candidate for the cause of LCM in SLs, and the standard model depicting the undulations is shown in Fig.

Report Documentation Page

Form Approved
OMB No. 0704-0188

1. REPORT DATE	2. REPORT TYPE	3. DATES COVERED
AUG 2002		**00-00-2002 to 00-00-2002**

4. TITLE AND SUBTITLE	5a. CONTRACT NUMBER
Lateral composition modulation in InAs/GaSb superlattices	5b. GRANT NUMBER
	5c. PROGRAM ELEMENT NUMBER
6. AUTHOR(S)	5d. PROJECT NUMBER
	5e. TASK NUMBER
	5f. WORK UNIT NUMBER
7. PERFORMING ORGANIZATION NAME(S) AND ADDRESS(ES) **Naval Research Laboratory,4555 Overlook Avenue SW,Washington,DC,20375**	8. PERFORMING ORGANIZATION REPORT NUMBER
9. SPONSORING/MONITORING AGENCY NAME(S) AND ADDRESS(ES)	10. SPONSOR/MONITOR'S ACRONYM(S)
	11. SPONSOR/MONITOR'S REPORT NUMBER(S)

12. DISTRIBUTION/AVAILABILITY STATEMENT
Approved for public release; distribution unlimited

13. SUPPLEMENTARY NOTES

14. ABSTRACT

15. SUBJECT TERMS

16. SECURITY CLASSIFICATION OF:			17. LIMITATION OF ABSTRACT	18. NUMBER OF PAGES	19a. NAME OF RESPONSIBLE PERSON
a. REPORT **unclassified**	b. ABSTRACT **unclassified**	c. THIS PAGE **unclassified**	**Same as Report (SAR)**	**5**	

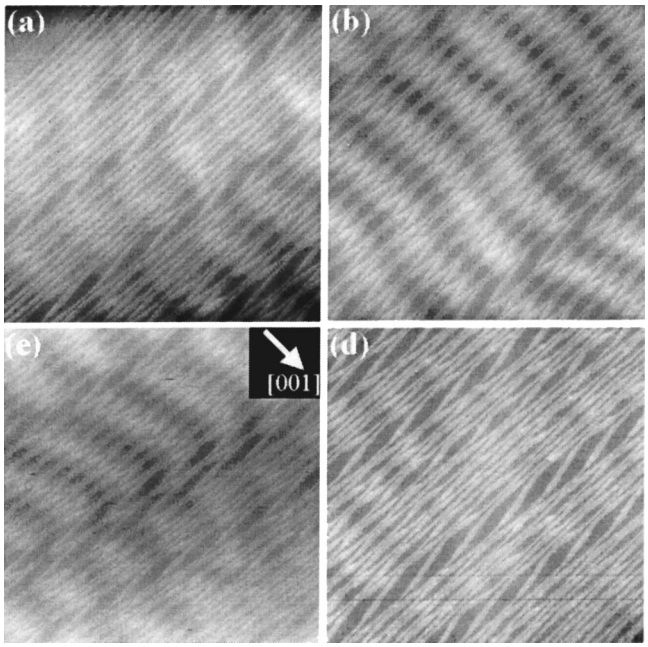

FIG. 1. XSTM image in the [110] projection for the entire vertical height of the 140 period $(InAs)_{13}/GaSb)_{13}$ superlattice where images of periods (a) 1–45, (b) 32–84, (c) 58–117, and (d) 84–137 are shown.

2(a).[17] The morphology observed in Fig. 1(b) is depicted schematically in Fig. 2(b), with the corresponding diffraction peaks in reciprocal space, and is quite different from the standard model. The thickest parts of the undulating layers A are offset from each other by half the undulation wavelength, resulting in a vertical period twice that of the deposited superlattice. This may occur in order for the layer to maintain the flattest, lowest energy surface possible. The parallelogram depicts the superstructure unit cell, corresponding to both the vertical and lateral structures. The shape of the unit cell is due to the stacking of the undulating layers. The tilt α of the unit cell base with respect to the (001) plane leads to an equal tilt of the vertical satellite peaks with respect to the [001] direction.

Although thickness undulations were observed in the XSTM image, this does not necessarily imply that chemical LCM exists. If the thickness of layer B in Fig. 2(b) does not vary, this structure will not exhibit LCM; the A/B ratio would be the same in regions *u* and *w*. On the other hand, if the thickness of layer B varies as depicted in Fig. 2(b), the A/B ratio is greater in regions *w* and smaller in regions *u*, resulting in LCM. The essentially vertical bright and dark stripes in Fig. 1, InAs-rich and GaSb-rich regions, respectively, imply that LCM is present. This was verified by XRD.

For periodic lateral structure, i.e., thickness undulation and composition modulation, the Bragg diffraction peaks are surrounded by a set of lateral satellites. If only thickness undulations are present, lateral satellites may be present about high order vertical satellites; however, only LCM will lead to lateral satellites about the zeroth order vertical satellite, SL0, which corresponds to the average SL lattice spacing. The effects of LCM on the SL0 peak itself may also be observable along the growth direction, depending on the magnitude of the composition change.

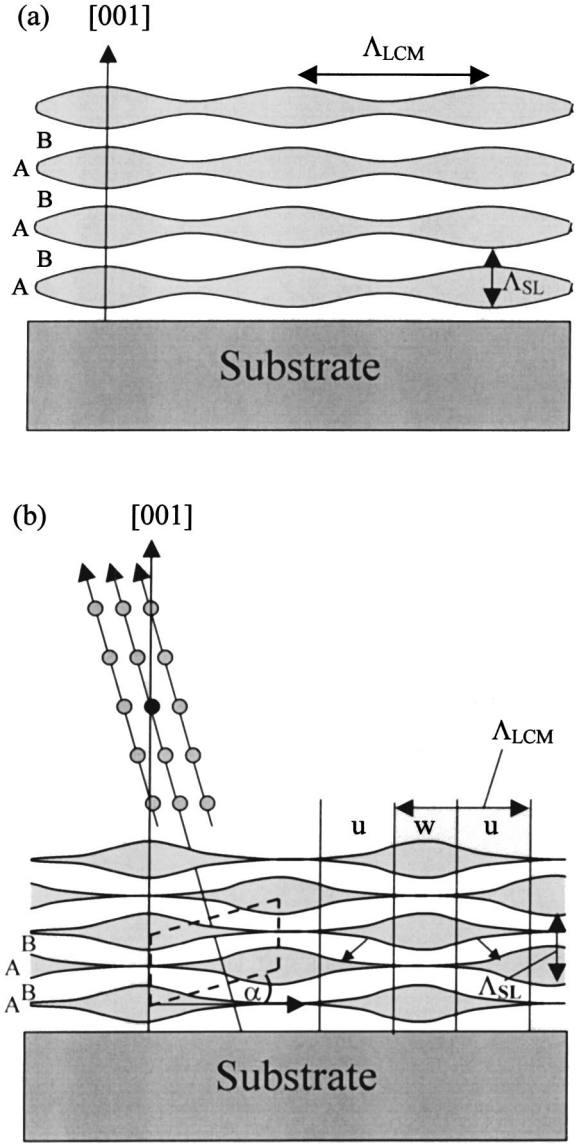

FIG. 2. Schematic diagrams of (a) predicted LCM in SPS structure and (b) the LCM observed in an $(InAs)_{13}/GaSb)_{13}$ superlattice, along with the associated diffraction pattern in reciprocal space. Λ_{SL} and Λ_{LCM} are the wavelengths of the vertical SL and LCM, respectively. Regions *u* and *w* represent Ga-rich and In-rich regions of the structure, respectively. The small arrows indicate where the GaSb (layer B) is thickest (between a trough and a crest of the InAs layer). The parallelogram shows the unit cell corresponding to the vertical and lateral superstructure, where α is the angle between the unit cell base and the (001) plane. The black circle represents a Bragg diffraction peak from the average lattice (SL0), while the gray circles represent vertical and lateral satellites.

High-resolution double crystal XRD analysis of the sample was performed on a four-circle diffractometer with a 12 kW rotating anode x-ray source, using Cu $K_{\alpha 1}$ radiation ($\lambda = 1.540\,51$ Å). Radial line scans were performed through the (002), (004), and (006) Bragg peaks as well as reciprocal space maps (RSMs) about the (004), (224), and (444) Bragg peaks in the plane perpendicular to the lateral modulations ($\phi \equiv 0°$) and parallel to the lateral modulations ($\phi \equiv 90°$).

Radial line scans through the (004) Bragg peak at $\phi = 0°$ and $\phi = 90°$ are shown in Figs. 3(a) and 3(b), respectively. Note that the odd numbered vertical satellite peaks are missing from Fig. 3(b), which will be explained later. The

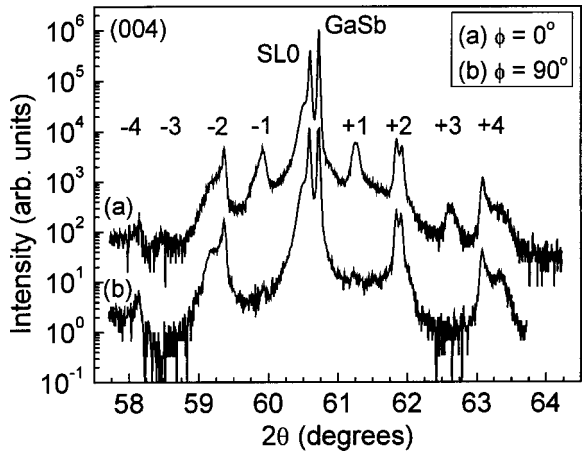

FIG. 3. XRD radial scans through the (004) Bragg peak at (a) $\phi = 0°$ and (b) $\phi = 90°$, which shows the absence of odd order satellites.

(004) RSM at $\phi = 0°$, Fig. 4, contains peaks corresponding to GaSb and the average superlattice (SL0), and vertical superlattice satellite peaks up to ± 2. The (224) and (444) RSMs indicate that the superlattice is fully strained to the GaSb substrate and buffer.

RSMs performed about the (004), (224), and (444) Bragg peaks at $\phi \equiv 90°$ confirmed the presence of LCM. The $\phi = 90°$ (004) and (444) RSMs are shown in Figs. 5(a) and 5(b), and show satellite peaks corresponding to both the vertical and lateral structure; lateral satellites are observed about the SL0 peak. In this plane, the vertical superlattice peaks are tilted with respect to [001], as depicted schematically in Fig. 2(b). The measured tilt of $7.5° \pm 0.5°$ does not affect the SL crystalline planes, i.e., the SL0 peak is not tilted with respect

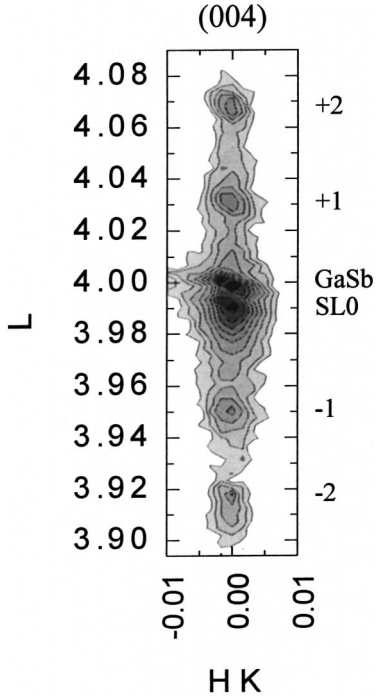

FIG. 4. XRD reciprocal space map around the (004) Bragg peak at $\phi = 0°$, perpendicular to the LCM, whose linear radial scan is shown in Fig. 3(a).

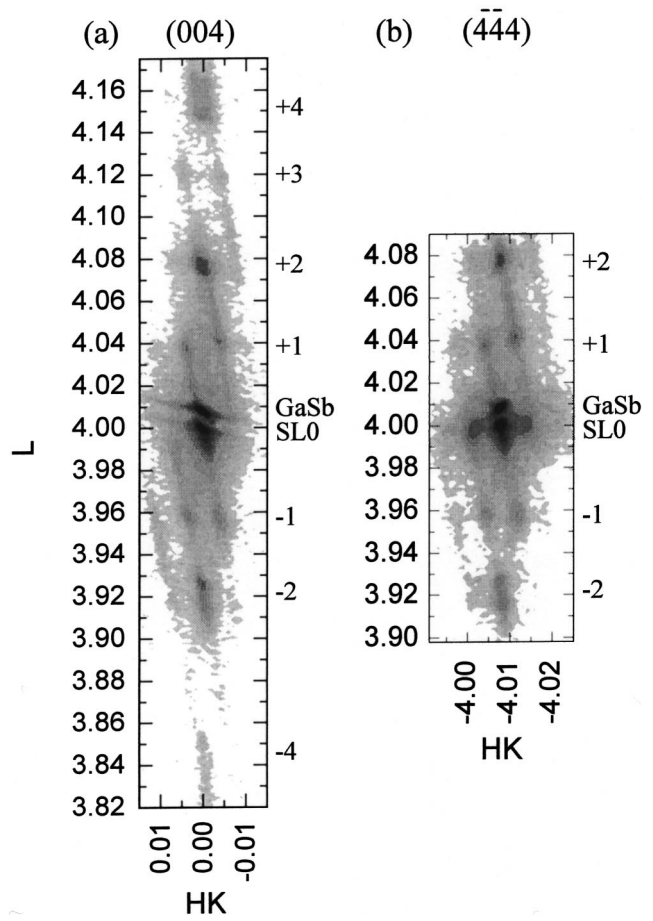

FIG. 5. XRD reciprocal space maps of LCM around the (a) (004) and (b) ($\bar{4}\bar{4}4$) Bragg peaks at $\phi = 90°$, parallel to the LCM, whose linear radial scan is shown in Fig. 3(b).

to the GaSb peak, and results from the stacking of the undulating layers. There are also diffuse streaks of intensity passing through the satellites along the stacking direction, which are naturally attributed to stacking errors. The vertical tilt explains the absence of the odd numbered satellites from the radial scan in Fig. 3(b); the odd numbered vertical satellite peaks are shifted off of the [001] axis in this plane, as seen in Figs. 5(a) and 5(b). Only two-dimensional RSMs can reveal both the LCM satellites and the tilting of the structure.

The LCM wavelength measured from the $\phi \equiv 90°$ RSMs, $\Lambda_{LCM} = 554 \pm 3$ Å, is in excellent agreement with the spacing measured between bright (or dark) columns in the XSTM image, which is approximately 600 Å. Note that XRD measurements average over the entire sampled volume, which in this case includes the entire vertical height of the sample, whereas XSTM images are highly localized. The thickness undulation wavelength measured from the XSTM images, assuming a sine wave periodicity, is 1100 $-$1200 Å, which is twice the LCM wavelength. Note that for a standard model LCM superlattice, Fig. 2(a), these two wavelengths would be identical. Typical LCM wavelengths reported in the literature range from 100 to 400 Å, which is similar to Λ_{LCM} for this sample.

The vertical SL wavelength, $\Lambda_{SL} = 155 \pm 10$ Å, was determined from all of the $\phi = 0°$ and $\phi = 90°$ RSMs and radial

scans. The intended SL wavelength was 80 Å. This measured doubling of the intended wavelength corresponds to the LCM structure as depicted in Fig. 2(b). The ± 10 Å variation of Λ_{SL} is best illustrated by the radial (004) scans in Fig. 3; the ± 2 and $+4$ satellite peaks show splitting. Unlike the work by Giannini *et al.*,[18] simulations indicate that the different compositions in regions *u* and *w* cannot completely account for the observed splitting. Rather, it indicates that there are two or more discrete Λ_{SL} values in the structure. We believe that this is due to variations along the growth direction, which are clearly seen in Fig. 1. This is consistent with the fact that the splitting is not seen in the odd numbered satellites which are due to the doubling of Λ_{SL} associated with the periodic lateral structure, and therefore come primarily from the sample section represented by Fig. 1(b). The entire sample contributes to the even numbered satellites, even where the lateral structure is weak, and therefore these will most strongly reflect variations along the growth direction.

The average SL lattice constant was determined from all of the scans, both at $\phi = 0°$ and 90°, and measured relative to GaSb which was assumed to be relaxed with $a = 6.0959$ Å. The measured SL lattice constants are $a = 6.0959$ Å (in-plane), and $c = 6.1080 \pm 0.001$ Å (out-of-plane). This indicates that the nominally InAs SL layers ($a_{InAs} = 6.0583$ Å) are in fact InAsSb. This is consistent with previous STM images of this sample that showed both Sb in the InAs layers as well as some As in the GaSb layers.[15] The complex structure of the sample prevented a complete fit of the XRD intensities, however, simulations indicated that the fraction of As in the GaSb layers is less than 4%, and that the fraction of Sb in the InAs layers varies from $\sim 12\%$ in regions *u* to $\sim 8\%$ in regions *w*, where InSb interfacial bonds have been considered. This alloying was not addressed in previous publications,[15,16] although it is consistent with XSTM images of the sample.

IV. DISCUSSION

While surface undulations have been observed in other samples,[19] this is the clearest image of thickness undulations in a SL exhibiting LCM. This is partly due to the fact that this is not a SPS, i.e., these layers are more than a few monolayers thick. Images of a similar structure have been obtained by cross-sectional transmission electron microscopy of InAs/AlInAs superlattices.[20] There have been no other reports of vertical wavelength doubling, indicative of the structure observed here; however, different undulation structures are likely to occur, depending on the strain between the SL layers and the substrate.[4–6,11,17,21–25]

Thickness undulations are clearly the cause of LCM in this sample. The InAs(Sb) layer thickness ranges from 4 to 28 monolayers, while the Ga(As)Sb thickness varies from 8 to 18 monolayers, as determined from XRD simulations. This leads to InAs(Sb)/Ga(As)Sb ratios of approximately 2:1 in region *w* and 1:3 in region *u*. There is alloying in the SL layers, and there is some lateral variation of the alloying, but this effect is much smaller than the large thickness variations that are observed.

The surprising lateral structure of this sample is attributed to the facts that (1) the Ga(As)Sb thickness undulations are much smaller than those of the InAs(Sb) layer, and (2) the thickest part of the Ga(As)Sb layer is not above a trough in the previous InAs(Sb) layer, but between a crest and trough. There are two possible explanations for the initial point. Thickness undulations are believed to be driven by strain relaxation.[11,21,26–30] This SL is fully strained, i.e., lattice matched to the GaSb substrate. The relaxed lattice constants corresponding to the limiting layer compositions given above are 6.1102 Å for $InAs_{0.877}Sb_{0.123}$ and 6.0767 Å for $GaAs_{0.043}Sb_{0.957}$. Thus, the InAs(Sb) layer is under a compressive strain $\leqslant 0.2\%$ and the Ga(As)Sb layer is a under tensile strain $\leqslant 0.3\%$. Although these strains are small, the InAs(Sb) is under compressive strain, which has been shown to be more likely to lead to film instabilities.[11,31–33] Second, the surface tensions of these layers are 1400 ergs/cm^2 for InAs, and 1600 ergs/cm^2 for GaSb. With alloying of the layers, the surface tension of InAs would decrease, while that of GaSb would increase. The somewhat smaller InAs(Sb) surface tension makes it more likely to form undulations. Although these influences are small, they would tend to cause greater thickness variation in the InAs(Sb) layer.

The position of the Ga(As)Sb ''crest'' does not appear to be explained by current elastic instability theory. Several articles have addressed the morphology of strained-layer superlattices, and predict elastic roughening or ripples as it is related to the growth mode.[11,21,26–30,34,35] The theory that most closely describes the observed LCM structure is by Shilkrot *et al.*[21] This theory predicts undulations, which are classified as an in-phase, complex or out-of-phase growth mode. In the in-phase mode, each sequential layer is modulated in-phase, with the amplitude of modulation increasing as the growth progresses. This structure does not lead to LCM. In the out-of-phase mode, each sequential layer is 180° out-of-phase with its surrounding layers, as depicted in our Fig. 2(a). SL layers A and B are assumed to be strain balanced with respect to the substrate, having equal and opposite strain. This theory predicts that an undulating layer will be most relaxed at its crests (lowest surface energy); hence, material B prefers to grow on the troughs of material A due to the stress/strain state resulting from the underlying interface. In the complex mode described by Shilkrot *et al.*, alternating layers are either in or out of phase, and the pattern may be periodic or aperiodic. While both the out-of-phase and complex modes can lead to LCM, they do not explain the structure observed here, i.e., the preferential growth of Ga(As)Sb between the InAs(Sb) troughs and crests, which would be referred to as 90° out-of-phase in the Shilkrot *et al.* terminology. Our structure consists of alternating layers that are 90° and 180° out-of-phase with the surrounding layers.

If the preferred growth of the Ga(As)Sb between a trough and crest of the InAs(Sb) layer is to be explained by strain, the InAs(Sb) troughs must have an in-plane lattice constant *less* than that of the substrate and the Ga(As)Sb. This is unlikely, since there is no driving force for a reduction of the InAs(Sb) lattice constant below that of Ga(As)Sb. In this case, the detailed surface diffusion and gradient en-

ergy contributions to the evolving structure must be considered.

Alternatively, this may be explained by GaSb growth on facetted surfaces. It has been shown that the growth rate of GaSb (by metalorganic molecular beam epitaxy) is enhanced on (11*n*) substrates over that on (001).[36] This may imply that the growth rates will also be enhanced at atomic steps consisting of (11*n*) planes. This sample was grown on a nominally (001) substrate and x-ray measurements indicate a miscut of less than 0.2°. However, even a small miscut introduces steps on the surface; therefore, the GaSb may grow at a faster rate on the step edges of the InAs layer, resulting in the observed stacking of the layers.

Finally, we discuss the tilt of the vertical peaks away from the [001] direction. This tilt should equal the tilt α [Fig. 2(b)] of the superstructure unit cell with respect to the (001) plane. The angle α is given by $\tan^{-1}(1/2\Lambda_{SL}/\Lambda_{LCM}) = 7.96°$ and is in excellent agreement with the $7.5° \pm 0.5°$ tilt measured from the RSMs. The diffuse streaks seen in Fig. 5 occur only along one tilt direction, which is attributed to a slight miscut of the substrate. The RSMs appear similar to those from LCM structures grown on intentionally miscut substrates, in which the tilt angle matches the miscut angle, even though the cause of the tilt is quite different.[37,38]

V. SUMMARY

In conclusion, we have reported the observation of LCM in an $(InAs)_m/(GaSb)_m$ SL and have shown a clear image of thickness undulations in a LCM sample. We identify thickness undulations as the cause of LCM in this structure. These undulations may be due to the strain state or surface tension of the layers or a combination of these effects, along with unequal surface diffusion of the species. Using XRD we have quantitatively described the morphology and structure of the sample. Because of its unconventional structure, no theoretical model is currently available that can explain the LCM formation.

In a parallel publication, the structure is described as an organization of InAs nanowires spontaneously formed within the InAs/GaSb superlattice.[16] We chose to describe this more conservatively as LCM because of the correlation of the InAs/GaSb regions. With control of the LCM formation, i.e., modulation wavelength, these structures may indeed prove to be useful for quantum wire applications.

ACKNOWLEDGMENTS

The authors would like to thank W. Donner for valuable discussions concerning fittings of the XRD data. This work was supported by the National Science Foundation on DMR-0099573, the Texas Center for Superconductivity and Advanced Materials (TcSAM) through the state of Texas and the University of Houston New Faculty Research Program. Research at the Naval Research Laboratory was supported by the Office of Naval Research and by the Defense Advanced Research Projects Agency.

[1] F. Peiro, A. Cornet, J. C. Ferrer, J. R. Morante, G. Halkias, and A. Georgakilas, Mater. Res. Soc. Symp. Proc. **417**, 265 (1996).
[2] R. D. Twesten, D. M. Follstaedt, E. J. Heller, E. D. Jones, S. R. Lee, J. M. Mullinchick, F. A. J. M. Driessen, and J. D. Mascarenhas, Bull. Am. Phys. Soc. **41**, 693 (1996).
[3] A. Mascarenhas, R. G. Alonso, G. S. Horner, S. Froyen, K. C. Hsieh, and K. Y. Cheng, Superlattices Microstruct. **12**, 57 (1992).
[4] K. C. Hsieh, J. N. Baillargeon, and K. Y. Cheng, Appl. Phys. Lett. **57**, 2244 (1990).
[5] J. M. Millunchick, R. D. Twesten, D. M. Follstaedt, S. R. Lee, E. D. Jones, Y. Zhang, S. P. Ahrenkiel, and A. Mascarenhas, Appl. Phys. Lett. **70**, 1402 (1997).
[6] K. Y. Cheng, K. C. Hsieh, and J. N. Baillargeon, Appl. Phys. Lett. **60**, 2892 (1992).
[7] Y. Zhang and A. Mascarenhas, Phys. Rev. B **57**, 12245 (1998).
[8] A. M. Moy, A. C. Chen, K. Y. Cheng, L. J. Chou, K. C. Hsieh, and C.-W. Tu, J. Appl. Phys. **80**, 7124 (1996).
[9] P. J. Pearah, A. C. Chen, A. M. Moy, K. C. Hsieh, and K. Y. Cheng, IEEE J. Quantum Electron. **30**, 608 (1994).
[10] D. E. Wohlert, K. Y. Cheng, and S. T. Chou, Appl. Phys. Lett. **78**, 1047 (2001).
[11] B. J. Spencer, P. W. Voorhees, and J. Tersoff, Phys. Rev. B **64**, 235318 (2001).
[12] C. Dorin and J. M. Millunchick, J. Appl. Phys. **91**, 237 (2002).
[13] M. J. Yang, W. J. Moore, B. R. Bennett, and B. V. Shanabrook, Electron. Lett. **34**, 270 (1998).
[14] F. Fuchs, U. Weimer, W. Pletschen, J. Schmitz, E. Aslswede, M. Walther, and J. Wagner, Appl. Phys. Lett. **71**, 3251 (1997).
[15] B. Z. Nosho, B. R. Bennett, L. J. Whitman, and M. Goldenberg, J. Vac. Sci. Technol. B **19**, 1626 (2001).
[16] B. Z. Nosho, B. R. Bennett, L. J. Whitman, and M. Goldenberg, Appl. Phys. Lett. (to be published).
[17] A. C. Chen, A. M. Moy, L. J. Chou, K. C. Hsieh, and K. Y. Cheng, Appl. Phys. Lett. **66**, 2694 (1995).
[18] C. Giannini, L. Tapfer, Y. Zhang, L. D. Caro, T. Marschner, and W. Stolz, Phys. Rev. B **55**, 5276 (1997).
[19] M. E. Twigg, B. R. Bennett, and R. Magno, J. Cryst. Growth **191**, 651 (1998).
[20] H. Li, T. Daniel-Race, and M. A. Hasan, J. Vac. Sci. Technol. B **19**, 1471 (2001).
[21] L. E. Shilkrot, D. J. Srolovitz, and J. Tersoff, Phys. Rev. B **62**, 8397 (2000).
[22] K. Y. Cheng, K. C. Hsieh, J. N. Baillargeon, and A. Mascarenhas, Proceedings of the 18th International Symposium on GaAs and Related Compounds, 1992, Vol. 120, p. 589.
[23] J. M. Millunchick et al., MRS Bull. **22**, 38 (1997).
[24] S. T. Chou, K. C. Hsieh, K. Y. Cheng, and L. J. Chou, J. Vac. Sci. Technol. B **13**, 650 (1995).
[25] R. S. Goldman, R. M. Feenstra, C. Silfvenius, B. Stålnacke, and G. Landgren, J. Vac. Sci. Technol. B **15**, 1027 (1997).
[26] D. J. Srolovitz, Acta Metall. **37**, 621 (1989).
[27] B. J. Spencer, P. W. Voorhees, and S. H. Davis, J. Appl. Phys. **73**, 4955 (1993).
[28] L. Shilkrot, D. J. Srolovitz, and J. Tersoff, Appl. Phys. Lett. **77**, 304 (2000).
[29] B. J. Spencer, S. H. Davis, and P. W. Voorhees, Phys. Rev. B **47**, 9760 (1993).
[30] J. E. Guyer and P. W. Voorhees, J. Cryst. Growth **187**, 150 (1998).
[31] Y. H. Xie et al., Phys. Rev. Lett. **73**, 3006 (1994).
[32] J. Tersoff, Phys. Rev. Lett. **74**, 4962 (1995).
[33] Y. H. Xie et al., Phys. Rev. Lett. **74**, 4963 (1995).
[34] J. H. Li, V. Holy, M. Meduna, S. C. Moss, A. G. Norman, A. Mascarenhas, and J. L. Reno, Phys. Rev. B **66**, 115312 (2002).
[35] J. H. Li et al., Appl. Phys. Lett. **78**, 219 (2001).
[36] K. Yamamoto, H. Asahi, K. Hidaka, J. Satoh, and S. Gonda, J. Cryst. Growth **179**, 37 (1997).
[37] V. Holy, U. Pietsch, and T. Baumbach, High-Resolution X-Ray Scattering from Thin Films and Multilayers (Springer, Berlin, 1999).
[38] C. Giannini et al., Phys. Rev. B **61**, 2173 (2000).